



Published in final edited form as:

*Transl Stroke Res.* 2010 September ; 1(3): 184–196. doi:10.1007/s12975-010-0016-6.

## Sublethal Transient Global Ischemia Stimulates Migration of Neuroblasts and Neurogenesis in Mice

**Ying Li,**

Department of Pathology and Laboratory Medicine, Medical University of South Carolina, Charleston, SC 29425, USA

**Shan Ping Yu,**

Department of Anesthesiology, Emory University School of Medicine, 101 Woodruff Circle, Suite 617, Atlanta, GA 30322, USA

**Osama Mohamad,**

Department of Anesthesiology, Emory University School of Medicine, 101 Woodruff Circle, Suite 617, Atlanta, GA 30322, USA

**Thomas Genetta,** and

Department of Neurology, Emory University School of Medicine, Atlanta, GA 30322, USA

**Ling Wei**

Department of Pathology and Laboratory Medicine, Medical University of South Carolina, Charleston, SC 29425, USA

Department of Anesthesiology, Emory University School of Medicine, 101 Woodruff Circle, Suite 617, Atlanta, GA 30322, USA

Department of Neurology, Emory University School of Medicine, Atlanta, GA 30322, USA

### Abstract

Increasing evidence has shown the potential of neuronal plasticity in adult brain after injury. Neural proliferation can be triggered by a focal sublethal ischemic preconditioning event; whether mild global ischemia could cause neurogenesis has been not clear. The present study investigated stimulating effects of sublethal transient global ischemia (TGI) on endogenous neurogenesis and neuroblast migration in the subventricular zone (SVZ), dentate gyrus, and peri-infarct areas of the adult cortex. Adult mice of 129S2/Sv strain were subjected to 8-min bilateral common carotid artery ligation followed by 5-bromo-2'-deoxyuridine (BrdU; 50 mg/kg, intraperitoneal) administration every day until being sacrificed at 1–21 days after reperfusion. The mild TGI did not induce neuronal cell death for up to 7 days after TGI, as evidenced by negative terminal deoxynucleotidyl transferase-mediated dUTP nick end labeling staining among NeuN-positive cells in the hippocampus and neocortex. In TGI animals, BrdU staining revealed enhanced proliferation of neuroblasts and their migration track from the SVZ into the striatum and neocortex. In the corpus callosum, there were more BrdU-positive cells in the TGI group in the first 2 days. Increasing numbers of BrdU-positive cells were seen 7–21 days later in the striatum and cortex of TGI mice. The cortex of TGI animals showed increased expression of erythropoietin, erythropoietin receptor, fibroblast growth factor 2, vascular endothelial growth factor, and phosphorylated Jun N-terminal kinase; the expression was peaked 2 to 3 days after reperfusion. BrdU and NeuN double staining in the dentate gyrus, striatum, and cortex implied

increased neurogenesis induced by the TGI preconditioning. Doublecortin (DCX)-positive cells increased in the cortex of TGI mice, localized to cortical layers II, III, and V, and many stained positive for the mature neuronal markers NeuN, neurofilament, N-methyl-D-aspartic acid receptor subunit gene NR1, or the gamma-aminobutyric-acid-synthesizing enzyme glutamic acid decarboxylase (GAD67). The atypical localization of DCX-positive cells and the colabeling with mature neuronal markers suggested that, in addition to indentifying migrating neuroblasts, DCX might also be a stress marker in the cortex. It is suggested that the sublethal TGI-induced regenerative responses may contribute to the beneficial effects of ischemic preconditioning.

### Keywords

Transient global ischemia; Neuroblasts; Neurogenesis; Cell migration; Doublecortin (DCX); Subventricular zone (SVZ)

---

### Introduction

During development, pluripotent neural stem cells of the pseudo-stratified neural tube have the ability to generate all of the cell types of the nervous system. Following their generation and under the control of preprogrammed and closely timed processes, these cells will migrate to precisely defined locations to form functional central nervous system (CNS) circuits. The migration patterns of neuroblasts from the ventricular and subventricular zones (SVZ) to specific cerebral cortex layers and the striatum have been well studied [1, 2]. In early investigations, Altman and Das showed that both the hippocampus and olfactory bulb (OB) have dividing cells that can become neurons in the postnatal rat brain [3, 4]. However, neurogenesis in the adult brain was not well studied, and it was a general consensus that injured brain could not regenerate and dead neuronal cells could not be replaced. More compelling evidence, however, supports that at least two CNS regions of the adult brain can be neurogenic: SVZ of the lateral ventricles that generates neural progenitor cells and forms rostral migratory stream to the OB [5] and the subgranular zone (SGZ) of the dentate gyrus (DG) in the hippocampal formation [6]. Under pathological conditions, SVZ cells are recruited and migrate to sites of injury, where they can contribute to subsequent tissue regeneration [7–10]. SGZ-derived cells are, likewise, stimulated by insults such as seizure and ischemia and can migrate over a short distances to integrate into the granule cell layer [11, 12]. It has subsequently been determined that injury-induced transient increases in plasticity in the adult CNS recapitulate events and patterns of gene expression observed during development [13].

Ischemic/hypoxic preconditioning is a powerful endogenous phenomenon where brief episodes of a subtoxic ischemic/hypoxic insult in vitro or in vivo induce robust protection against future severe insults [14–17]. Exposure to sublethal ischemia/hypoxia alters gene expression and activates intracellular signaling pathways involved in cell survival and regenerative processes. These changes may contribute to the adaptive responses observed after ischemic injury. Hypoxia can prolong the half-life of several mRNAs, such as HIF-1 $\alpha$ , vascular endothelial growth factor (VEGF), and erythropoietin (EPO) [18, 19]. In addition to the protective effects, preconditioning with a focal sublethal ischemia also stimulates cell proliferation, differentiation, angiogenesis, and neurogenesis in the CNS [20–22]. Whether a global ischemic preconditioning causes increased neural cell proliferation and neurogenesis in the adult brain has not been well defined.

Transient global ischemia (TGI), caused by cardiac arrest in humans and induced in animals such as gerbils, rats, and sensitive strains of mouse by bilateral occlusion of the common carotid arteries (CCA), typically results in neuronal cell death in the hippocampus, an area

of the brain highly vulnerable to hypoxia/ischemia insult. The rodent TGI models have been used to explore postinjury neurogenesis [23, 24].

However, only limited studies have employed TGI to investigate the proliferation, migration, and differentiation of SVZ-derived adult neuroblasts [25], and most of them have focused on the effect of lethal insults. In the present investigation, instead of focusing on cell death and tissue injury, we investigated whether a sublethal TGI was strong enough to stimulate neuroblast migration and endogenous neurogenesis. Such sublethal TGI may serve as a trigger for the well-known phenomenon of ischemic preconditioning. A better understanding of the sublethal insult on endogenous neurogenesis is expected to provide insight into the regenerative mechanism of ischemic preconditioning.

## Materials and Methods

### Sublethal Transient Global Ischemia

All animal experiments and surgery procedures were approved by the University Animal Research Committee and meet NIH standards. Male 129S2/Sv mice (25–30 g, Charles River Laboratories, Inc. Wilmington, MA, USA) were used to induce TGI. Briefly, animals were subjected to 4% chloral hydrate intraperitoneal (i.p.) anesthesia. The body temperature was maintained at  $37.0\pm 0.5^{\circ}\text{C}$  with heating pads, and rectal temperature was monitored throughout the surgery procedure. After midline neck incision, the bilateral CCA were carefully exposed and occluded with 6-0 suture (Surgical Specialties Co., Reading, PA, USA). The sutures were removed after 8 min for reperfusion. After wound closure, the mice were placed in an incubator set at  $33.0^{\circ}\text{C}$  and 50% humidity. They were returned to their cages after they were fully recovered from anesthesia. The sham group was performed with the same procedure including anesthesia and all surgical procedures, except the CCA occlusion. For mitotic labeling of cell proliferation, 5-bromo-2'-deoxyuridine (BrdU, Sigma, St. Louis, MO, USA) was administered (i.p.) to animals at a dosage of 50-mg/kg body weight after reperfusion and once daily until the day of sacrifice. Animals were sacrificed by decapitation at different days after reperfusion. The brain was immediately removed and mounted in optimal cutting temperature compound (Sakura Finetek USA, Inc., Torrance, CA, USA) at  $-80^{\circ}\text{C}$  for further processing.

### Cerebral Blood Flow Measurement

The cerebral blood flow (CBF) was measured on both sides of the hemisphere to evaluate blood supply in the cerebral cortex before, during, and after CCA occlusion by using laser Doppler scanning imaging. The measurements and analysis were performed by using the PeriScan® system and LDPIwin 2® (Perimed AB, Stockholm, Sweden).

### Terminal Deoxynucleotidyl Transferase-Mediated dUTP Nick End Labeling Staining

A terminal deoxynucleotidyl transferase-mediated dUTP nick end labeling (TUNEL) staining kit (DeadEnd™ Fluorometric TUNEL system, Promega, Madison, WI, USA) was used to visualize cell death in 10- $\mu\text{m}$  coronal frozen sections together with NeuN. After 10-min fixing by 10% buffered formalin phosphate (Fisher Scientific, Pittsburgh, PA, USA) and pretreatment with  $-20^{\circ}\text{C}$  ethanol/acetic acid (2:1) and 0.2% Triton X-100, the brain sections were incubated in an equilibration buffer as instructed by the kit. The TdT enzyme and nucleotide mix were then added at proportions specified by the kit for 75 min at room temperature. The slides were washed with the provided  $2\times$  SSC washing buffer. To identify neuronal death, slides were then incubated with the NeuN primary antibody (1:250, Chemicon, Temecula, CA, USA) overnight. After phosphate-buffered saline (PBS) washes and incubation with Cy3-conjugated antimouse immunoglobulin G (IgG; 1:1,000, Jackson ImmunoResearch, West Grove, PA, USA), the slides were incubated in Hoechst 33342

(1:20,000, Molecular Probes, Carlsbad, CA, USA) for 5 min to stain the nucleus before being mounted with ProLong Antifade mounting medium (Molecular Probes, Carlsbad, CA, USA) for observation.

### Immunofluorescence Staining

Coronal fresh frozen sections of 10  $\mu\text{m}$  thick were sliced using a cryostat Vibratome (Ultapro 5000; St. Louis, MO, USA). After the slides were completely air-dried, slices were fixed in 10% buffered formalin phosphate for 10 min, followed by treatments in a  $-20^{\circ}\text{C}$  ethanol/acetic acid (2:1) solution for 12 min, in 0.2% Triton-100 for 5 min and washed by PBS three times between each step. Slides were blocked in 1% gelatin from cold water fish (Sigma, St. Louis, MO, USA), diluted in PBS at room temperature for 1 h, and subsequently incubated with primary antibodies diluted in PBS overnight at  $4^{\circ}\text{C}$ . The primary antibodies were as follows: mouse anti-NeuN (1:250, Chemicon, Temecula, CA, USA), goat antidoublecortin (anti-DCX, 1:50, Santa Cruz Biotechnology, Santa Cruz, CA, USA), mouse anti-neurofilament (anti-NF, 1:1,000, Cruz Biotechnology, Santa Cruz, CA, USA), rabbit anti-N-methyl-D-aspartic acid (NMDA) receptor type 1 (NR1, 1:100, Affinity BioReagents, Golden, CO, USA), and rabbit anti-GAD67 (1:200, Santa Cruz Biotechnology, Santa Cruz, CA, USA). After rinsing with PBS, brain sections were then treated with secondary antibodies Alexa Fluor 488 anti-goat IgG (1:200, Molecular Probes, Carlsbad, CA, USA), Cy3-conjugated donkey antirabbit IgG, goat antimouse IgG (Jackson ImmunoResearch, West Grove, PA, USA), or Cy5-conjugated donkey antimouse IgG (Jackson ImmunoResearch, West Grove, PA, USA) for 1.5 h at room temperature. Hoechst 33342 was applied to stain all the nuclei as a background staining whenever it was necessary.

To double stain DCX with BrdU, slides were postfixated and the BrdU staining procedure was performed with rat anti-BrdU (1:500, Abcam, Cambridge, UK) and Cy3-conjugated goat antirat IgG (Jackson ImmunoResearch, West Grove, PA, USA) as the primary and secondary antibodies according to our established technique [26].

The brain sections were mounted and coverslipped and imaged and photographed under a fluorescent microscope (BX51, Olympus, Japan) and laser scanning confocal microscopy (Carl Zeiss Microimaging, Inc., Thornwood, NY, USA).

### Systematic Histological Quantification

For systematic random sampling in design-based cell counting, every ninth brain sections (90  $\mu\text{m}$  apart) across the entire region of interest were counted. To count BrdU-positive cells in DG, four fields per brain section were randomly chosen under  $\times 40$  magnification of a light microscope or in confocal images. This was repeated in four separate sections per brain ( $n=6$  per group). For counting the DCX-positive cells in neocortex and BrdU-positive cells in septum, striatum, corpus callosum, and neocortex, a fluorescent confocal microscope was set to  $\times 20$  magnification, and all the immune positive cells have been counted in the particular regions ( $n=6$  per group). Counts are expressed as the average cell number per field  $\pm$  standard error (SE) of means.

### Western Blot Assay of Neurogenic Factors

Expression of neurogenic proteins was examined by Western blot. Cortex tissue samples of both side hemispheres were collected, and proteins were extracted using the NE-PER Nuclear and Cytoplasmic Extraction Kit (Pierce Biotechnology, Rockford, IL, USA). Protein concentrations were determined by BCA assay (PIERCE, Rockford, IL, USA). The samples were kept frozen at  $-80^{\circ}\text{C}$  until assaying.

Samples of 50 µg proteins were electrophoresed on a 6–15% gradient gel in the presence of SDS–PAGE in a Hoefer Mini-Gel system (Amersham Biosciences, Piscataway, NJ, USA) and transferred in the Hoefer Transfer Tank (Amersham Biosciences, Piscataway, NJ, USA) to a PVDF membrane (Bio-Rad, Hercules, CA, USA). Membranes were blocked with buffer (Tris-buffered saline containing 0.1% Tween-20 (TBS-T), pH7.6, 7% milk) at room temperature for 2 h and incubated overnight at 4°C with rabbit polyclonal EPO (H-162), rabbit polyclonal erythropoietin receptor (EPOR; M-20), and rabbit polyclonal fibroblast growth factor 2 (FGF-2; 147; 1:1,000, Santa Cruz Biotechnology, Santa Cruz, CA, USA), anti-VEGF, clone JH121 (1:1,000, Upstate, Charlottesville, VA, USA), and rabbit antimouse Jun N-terminal kinase (JNK; 1:1,000, Cell Signaling, Danvers, MA, USA). Mouse β-actin antibody (Sigma, St. Louis, MO, USA) was used for protein loading control. The blots were washed in 0.5% TBS-T and incubated with alkaline phosphatase-conjugated antirabbit or antimouse IgG (Promega, Madison, WI, USA) for 2 h at room temperature. Finally, membranes were washed with TBS-T followed by three washes with TBS. Signal was detected by the addition of BCIP/NBT solution (Sigma, St. Louis, MO, USA), quantified and analyzed by the imaging software Photoshop Professional (Adobe Photoshop CS 8.0, San Jose, CA, USA).

### Statistical Analysis

Student's two-tailed *t* test was used for the comparison of two experimental groups. Multiple comparisons were done using one-way ANOVA followed by Tukey test for multiple pairwise examinations. Changes were identified as significant if *p* was less than 0.05. Mean values were reported together with the standard error of the mean.

## Results

### Sublethal TGI in Adult Mice

Sublethal TGI was induced via bilateral occlusion of the CCAs for 8 min. Laser Doppler scanning imaging and laser Doppler probe were used to monitor CBF before and after bilateral CCA occlusion (Fig. 1a, b). Animals with 60–70% reduction of CBF in both hemispheres were used in subsequent investigations. At 1 and 7 days after the TGI, brain sections were subjected to triple immunostaining of TUNEL, NeuN, and Hoechst 33342 to detect neuronal cell death. Under our experimental condition, the 8-min TGI insult induced few (0–3) TUNEL-positive cells in the neocortex and hippocampus sections from both hemispheres (Fig. 1c–e). This was in sharp contrast to massive cell death detected after a lethal ischemic insult (11-min bilateral CCA occlusion; Fig. 1, inset). We therefore judged that the 8-min TGI insult in this investigation was sublethal to neuronal cells.

### Sublethal TGI Enhances Proliferation of SVZ Neuroblasts and Induces Their Migration to the Neocortex

The proliferation marker BrdU was used to trace migration tracks of SVZ-derived cells. The number of BrdU-positive cells in a given region surrounding the SVZ, e.g., septum, striatum, and corpus callosum, was compared between TGI and sham groups. One to 2 days after TGI, more BrdU-positive cells appeared in the septum and corpus callosum compared with sham control animals. The increase of proliferating cells in these areas, however, was relatively transient. By 14 days after TGI, there was no longer a difference in BrdU-positive cells in septum. Moreover, the number of BrdU-positive cells in the corpus callosum was even less than in the sham-operated controls. On the other hand, BrdU-positive cells in striatum and neocortex increased in a delayed fashion; more and more new cells were seen in these two regions 3 and 14 days after TGI (Fig. 2). These data suggested a migration pattern of newly generated cells from the SVZ area, passing through the white matter corpus callosum, and eventually reaching the striatum and cortex a few days later.

### **Sublethal TGI Upregulated the Expression of Neurotrophic Factors**

Western blot analysis was used to detect the expression of the neurotrophic and neurogenic factors EPO, EPOR, basic fibroblast growth factor 2, and VEGF in the neocortex 1–7 days after TGI. All four proteins were upregulated in the TGI group compared with that in the sham-operated group (Fig. 3a). Within TGI groups, the induction of these factors peaked at the second (EPO and VEGF) or third (EPOR and FGF-2) day after reperfusion. The expression of EPO and FGF-2 was higher compared to the expression of EPOR and VEGF (Fig. 3b–e), while there were no obvious changes in the sham-operation groups.

### **Sublethal TGI Activates Jun N-terminal Kinase Phosphorylation**

Phosphorylation levels of JNK in the neocortex were detected using Western blot. JNK was dramatically phosphorylated 3 days after TGI and returned to normal levels by 7 days in the sublethal TGI group (Fig. 4).

### **Sublethal TGI Enhances the Neural Plasticity in the Dentate Gyrus, Striatum, and Neocortex**

In the sublethal TGI model, proliferation and neurogenesis were assessed using BrdU staining and BrdU/NeuN double staining. One day after reperfusion, more BrdU-positive cells were observed in the DG (on both sides) in the TGI group compared to those in sham controls (Fig. 5a, b). Within TGI groups, the numbers of BrdU-positive cells at 7, 14, and 21 days were significantly higher than those from 1, 2, and 3 days after reperfusion (Fig. 5g). BrdU/NeuN-double-positive cells were first seen 7 days after reperfusion (Fig. 5c–f). The number of these double-positive cells was significantly higher in the TGI group than in the sham group 7, 14, and 21 days after reperfusion.

### **Sublethal TGI Activates Transient Expression of DCX in the Neocortex**

Immunohistochemistry was used to detect the expression of DCX in the neocortex. Interestingly, most of the DCX-positive cells were localized to cortical layers II, III, and V (Fig. 6e, f). In the TGI group of 1 to 14 days following reperfusion, there were more DCX-positive cells in both hemispheres of the neocortex compared to the sham group where DCX-positive cells are much less detectable; these numbers in TGI animals decreased rapidly to sham levels 21 days after reperfusion (Fig. 6d). Double or triple immunohistochemical staining for mature neuronal markers NeuN, NF, NR1, and GAD67 detected colocalization of these markers with DCX in the neocortex (Figs. 6a–c and 7).

## **Discussion**

The present investigation demonstrates adult neurogenesis following sublethal TGI in 129S2/Sv adult mice. The sublethal TGI provides a model of global ischemic preconditioning, which has been less studied, and its stimulating effect on neural regeneration has been poorly understood. We show that sublethal TGI enriches the neocortical microenvironment by upregulating the expression of neurotrophic factors including EPO, EPOR, FGF-2, and VEGF. We further show that enhanced neuronal regeneration and/or plasticity after sublethal TGI not only occurs in the SVZ and hippocampus (DG) but also in the striatum and neocortex. Finally, to the best of our knowledge, this is the first report demonstrating that sublethal TGI can transiently upregulate DCX expression in the neocortex that may not be associated with migrating cells.

TGI diminishes cerebral blood flow over the entire brain. The clinical correlation of TGI (systemic hypoperfusion) occurs in patients suffering from cardiac arrest, shock, or undergoing complex cardiac surgery [27, 28]. Global ischemic insults can manifest in a broad range of neurological dysfunction, such as cognitive deficits. The reduction in

cerebral blood flow from its normal range (from 50 to 75 ml/100 g of brain tissue per minute to around 18 ml per 100 kg/min) will precipitate significant cellular depolarization. Animal models have been developed to study mechanisms of neurological damage and (critical for clinical practice) to identify potential targets for cytoprotective strategies. The most commonly used model of global ischemia is induced in rodents by transient bilateral CCA occlusion. The extent of injury can be adjusted by the duration of the CCA occlusion. Specific neuronal populations in this animal model are susceptible to injury, the neurons in the CA1 zone of hippocampus being the most vulnerable to depolarizing ischemia. The TGI model has, therefore, been primarily used to investigate mechanisms of hippocampal neuronal injury and cell death. The amount of CCA occlusion required for the induction of TGI is also strain dependant. Most of the studies in mice have used the C57BL/6 strain. There are fewer reports describing the effects of TGI on 129S2/Sv mice, largely because this strain has been thought to be resistant to ischemic injury [29, 30]. In our study, we took the advantage of the relative ischemic tolerance of 129S2/Sv mice and established a stable TGI preconditioning model in these mice. The reduction in CBF was monitored using laser Doppler scanning and/or a laser Doppler probe, which are well-established techniques for CBF measurements [31]. The criterion for stable sublethal TGI has been set as 60–70% reduction in CBF. In this mouse strain, this amount of CBF reduction did not cause noticeable cell death. Work from Moskowitz's group demonstrated that although there were no significant differences in anterior and middle segments of the circle of Willis between C57Black/6 mice and Sv-129 mice, larger posterior communicating arteries were detected in Sv-129 mice than in C57Black/6 mice. This difference could well be responsible for the higher tolerance of Sv-129 mice to brain ischemia [32].

The TUNEL assay was used to detect cell death 1 and 7 days after reperfusion. There was no noticeable increase in the number of TUNEL-positive cells in either the neocortex or hippocampus. These data satisfy our goal of testing the effect of sublethal TGI on endogenous regenerative responses. It is worth noticing that even if there is no detectable cell death induced by the TGI, the ischemic insult evidently imposes significant stress on the brain especially to vulnerable hippocampal neurons and likely to the regions involved in neurogenesis such as SVZ.

Ischemic/hypoxic preconditioning is a powerful endogenous protective mechanism that normally triggers upregulation of trophic/growth factors and shows acute (within minutes or hours) and prolonged (up to days and even weeks) cytoprotective effects. Most previous investigations in the brain have been focused on the neuroprotective action of ischemic preconditioning. Only a handful of studies have reported a promoting effect of ischemic/hypoxic preconditioning on neurogenesis. A few recent reports show that focal ischemia induced by middle cerebral artery occlusion stimulates neurogenesis in the SVZ [33, 34]. One early study showed that 10-min bilateral CCA of adult gerbils caused 12-fold increases in cell proliferation in the dentate subgranular zone 1–2 weeks after reperfusion [35]. Identified with neuronal markers, newborn neurons were first seen 26 days after ischemia and survived for at least 7 months. In the current investigation, we observed enhanced cell proliferation a few days into reperfusion; the newborn cells could be identified up to 21 days later. The difference in the timing of neurogenesis may be due to the differences in animal species tested in these investigations (gerbil vs. mouse). The long survival of newly generated cells suggests that these cells might be able to contribute to tissue repair and regeneration. This is consistent with a recent report showing that suppression of proliferating progenitor cells blocks the induction of ischemic tolerance [36].

After sublethal TGI, neural precursors in the SVZ were activated. Three regions surrounding the SVZ, the septum, striatum, and corpus callosum, as well as the neocortex, were selected to examine the migration of recruited neuro-blasts after TGI [8, 37]. Our results reveal

several interesting differences in the numbers of BrdU-positive cells between these regions. We observed that there were significantly more BrdU-positive cells in the area proximate to SVZ such as the septum of the TGI group 2 days after reperfusion, while increased BrdU-positive cells were seen several days later in the striatum and cortex. The neocortex is connected to the SVZ by the corpus callosum. The numbers of BrdU-positive cells in corpus callosum of the TGI group increased within the first 2 days after reperfusion but decreased in later days. This is consistent with the idea that SVZ-derived neuroblasts pass through the corpus callosum during the first few days and migrate into the striatum and cortex. Although our study did not distinguish cell types of BrdU-positive cells in the corpus callosum and some of those cells might be glial lineage cells, we did show that many BrdU-positive cells were NeuN positive in the DG and double labeling of NeuN/DCX in several brain regions, supporting the idea of neurogenesis. During development, neurons initially migrate from their place of birth to the intermediate zone (IZ), the future white matter in the mature brain. When they reach the IZ, these cells face a developmental fork: they will either continue following the path demarcated by radial glia to enter the cortical plate or migrate tangentially and distribute themselves laterally to other cortical regions [38]. The same migrating pattern of cells from the SVZ was observed during TGI-induced cell proliferation and migration. We hypothesize that the initial migration of the activated SVZ neuroblasts into the corpus callosum occurs in the relative absence of guidance cues. After a period of 3 days, the cells which have accumulated in the corpus callosum then receive appropriate signals, triggering their migration towards the neocortex.

To begin to investigate the nature of these neocortical migratory cues, we examined the changes in expression of a subset of neurotrophic factors, as well as migration-associated proteins. Protein levels of EPO, EPOR, FGF, and VEGF were upregulated 1 day after reperfusion and peaked by the second or third days, suggesting that the microenvironment in the neocortex was primed by the TGI insult. This unique post-TGI microenvironment in the neocortex may play a role in establishing the migratory cues attracting the proliferating neuroblasts. In addition to neurotrophins, we examined protein levels of c-JNK, a regulator of cell migration [32]. Inhibiting JNK affects the migration of several different cell types [39, 40]. In our study compared to controls, p-JNK was induced in the neocortex in the TGI animals and peaked by the third day. It is suggested, therefore, that sublethal TGI primes the neocortical microenvironment by upregulating the expression of several neurotrophic factors and migration-associated proteins. We recognize, however, that the present investigation was not aimed to demonstrate a causal relationship between detected upregulation of trophic factors and increased neurogenesis. Based on widely accepted conscience, it is possible that the observed increases of the trophic/growth factors may directly or indirectly promote the post-TGI neurogenesis and cell migration.

DCX is regarded as a marker for migrating neuroblasts and may participate in some neuronal plastic phenomena, such as neurite outgrowth and synaptogenesis [41, 42]. Many studies have shown that DCX can be used as a convenient marker to label neurogenesis [43], most of these were limited to areas surrounding the SVZ and DG [37, 44, 45]. DCX has also been used to follow stroke-induced neurogenesis as well as the migration of neuronal precursors toward the infarct boundary in the striatum [7]. The existence of DCX-positive cells resident in the neocortex, as opposed to those that accumulate from insult-mediated migration into this region, that also express mature neuron-specific markers was first mentioned by Nacher [46]. The significance of DCX-positive cells in the neocortex has been poorly understood. We show here via immunostaining that DCX-positive cells are present in the neocortex. Compared to sham controls, there were more DCX-positive cells in the neocortex 1 day after TGI. These numbers on both sides of the neocortex increased in the following days and, 14 days after reperfusion, peaked at 2.5 times the numbers seen in the



sham group. More importantly, the DCX-positive cells in the neocortex were not BrdU positive, suggesting that they could not be recently generated cells.

In order to better characterize DCX-positive cells in the neocortex, we double-stained for the well-established mature neuronal markers NeuN and NF. All DCX-positive cells in the neocortex colocalized with both NeuN and NF, suggesting that a well-developed neuronal/axonal network had been established. A subset of DCX-positive cells expressed the glutamatergic neuronal marker NR1 or the gamma-aminobutyric-acid (GABA)ergic neuronal marker GAD67, providing further evidence that at least some of these cells were differentiated mature neurons. The DCX-positive cells were significantly increased in the cortex just 1 day after TGI, a time point when SVZ-derived cells unlikely reached this area and differentiated into mature neurons. It appears that DCX may participate in the stress response after sublethal TGI. We suggest that more comprehensive evaluations of DCX-positive cells are needed to identify migrating activity in the postinjury/poststress brain.

## Acknowledgments

This work was supported by NIH grants NS37372, NS045155, and NS045810 and the American Heart Association and Bugher Foundation (AHA-Bugher) Awards 0170064 N and 0170063 N.

## References

1. Nadarajah B, Parnavelas JG. Modes of neuronal migration in the developing cerebral cortex. *Nat Rev Neurosci.* 2002; 3:423–432. [PubMed: 12042877]
2. Hamasaki T, Goto S, Nishikawa S, Ushio Y. Neuronal cell migration for the developmental formation of the mammalian striatum. *Brain Res Brain Res Rev.* 2003; 41:1–12. [PubMed: 12505644]
3. Altman J. Autoradiographic and histological studies of postnatal neurogenesis. IV. Cell proliferation and migration in the anterior forebrain, with special reference to persisting neuro-genesis in the olfactory bulb. *J Comp Neurol.* 1969; 137:433–457. [PubMed: 5361244]
4. Altman J, Das GD. Autoradiographic and histological evidence of postnatal hippocampal neurogenesis in rats. *J Comp Neurol.* 1965; 124:319–335. [PubMed: 5861717]
5. Reynolds BA, Weiss S. Generation of neurons and astrocytes from isolated cells of the adult mammalian central nervous system. *Science.* 1992; 255:1707–1710. [PubMed: 1553558]
6. Gage FH. Mammalian neural stem cells. *Science.* 2000; 287:1433–1438. [PubMed: 10688783]
7. Zhang R, Zhang Z, Wang L, Wang Y, Goussev A, Zhang L, et al. Activated neural stem cells contribute to stroke-induced neurogenesis and neuroblast migration toward the infarct boundary in adult rats. *J Cereb Blood Flow Metab.* 2004; 24:441–448. [PubMed: 15087713]
8. Sundholm-Peters NL, Yang HK, Goings GE, Walker AS, Szele FG. Subventricular zone neuroblasts emigrate toward cortical lesions. *J Neuropathol Exp Neurol.* 2005; 64:1089–1100. [PubMed: 16319719]
9. Jin K, Sun Y, Xie L, Peel A, Mao XO, Bateur S, et al. Directed migration of neuronal precursors into the ischemic cerebral cortex and striatum. *Mol Cell Neurosci.* 2003; 24:171–189. [PubMed: 14550778]
10. Arvidsson A, Collin T, Kirik D, Kokaia Z, Lindvall O. Neuronal replacement from endogenous precursors in the adult brain after stroke. *Nat Med.* 2002; 8:963–970. [PubMed: 12161747]
11. Parent JM, Yu TW, Leibowitz RT, Geschwind DH, Sloviter RS, Lowenstein DH. Dentate granule cell neurogenesis is increased by seizures and contributes to aberrant network reorganization in the adult rat hippocampus. *J Neurosci.* 1997; 17:3727–3738. [PubMed: 9133393]
12. Jin K, Minami M, Lan JQ, Mao XO, Bateur S, Simon RP, et al. Neurogenesis in dentate subgranular zone and rostral subventricular zone after focal cerebral ischemia in the rat. *Proc Natl Acad Sci U S A.* 2001; 98:4710–4715. [PubMed: 11296300]

13. Emery DL, Royo NC, Fischer I, Saatman KE, McIntosh TK. Plasticity following injury to the adult central nervous system: is recapitulation of a developmental state worth promoting? *J Neurotrauma*. 2003; 20:1271–1292. [PubMed: 14748977]
14. Murry CE, Jennings RB, Reimer KA. Preconditioning with ischemia: a delay of lethal cell injury in ischemic myocardium. *Circulation*. 1986; 74:1124–1136. [PubMed: 3769170]
15. Bruer U, Weih MK, Isaev NK, Meisel A, Ruscher K, Bergk A, et al. Induction of tolerance in rat cortical neurons: hypoxic preconditioning. *FEBS Lett*. 1997; 414:117–121. [PubMed: 9305743]
16. Bolli R. The late phase of preconditioning. *Circ Res*. 2000; 87:972–983. [PubMed: 11090541]
17. Prass K, Scharff A, Ruscher K, Lowl D, Muselmann C, Victorov I, et al. Hypoxia-induced stroke tolerance in the mouse is mediated by erythropoietin. *Stroke*. 2003; 34:1981–1986. [PubMed: 12829864]
18. Jones NM, Bergeron M. Hypoxic preconditioning induces changes in HIF-1 target genes in neonatal rat brain. *J Cereb Blood Flow Metab*. 2001; 21:1105–1114. [PubMed: 11524615]
19. Paulding WR, Czyzyk-Krzeska MF. Hypoxia-induced regulation of mRNA stability. *Adv Exp Med Biol*. 2000; 475:111–121. [PubMed: 10849653]
20. Chong ZZ, Kang JQ, Maiese K. Hematopoietic factor erythropoietin fosters neuroprotection through novel signal transduction cascades. *J Cereb Blood Flow Metab*. 2002; 22:503–514. [PubMed: 11973422]
21. Buemi M, Cavallaro E, Floccari F, Sturiale A, Aloisi C, Trimarchi M, et al. The pleiotropic effects of erythropoietin in the central nervous system. *J Neuropathol Exp Neurol*. 2003; 62:228–236. [PubMed: 12638727]
22. Studer L, Csete M, Lee SH, Kabbani N, Walikonis J, Wold B, et al. Enhanced proliferation, survival, and dopaminergic differentiation of CNS precursors in lowered oxygen. *J Neurosci*. 2000; 20:7377–7383. [PubMed: 11007896]
23. Kawai T, Takagi N, Miyake-Takagi K, Okuyama N, Mochizuki N, Takeo S. Characterization of BrdU-positive neurons induced by transient global ischemia in adult hippocampus. *J Cereb Blood Flow Metab*. 2004; 24:548–555. [PubMed: 15129187]
24. Tanaka R, Yamashiro K, Mochizuki H, Cho N, Onodera M, Mizuno Y, et al. Neurogenesis after transient global ischemia in the adult hippocampus visualized by improved retroviral vector. *Stroke*. 2004; 35:1454–1459. [PubMed: 15073392]
25. Tonchev AB, Yamashima T, Sawamoto K, Okano H. Enhanced proliferation of progenitor cells in the subventricular zone and limited neuronal production in the striatum and neocortex of adult macaque monkeys after global cerebral ischemia. *J Neurosci Res*. 2005; 81:776–788. [PubMed: 16047371]
26. Li WL, Yu SP, Ogle ME, Ding XS, Wei L. Enhanced neurogenesis and cell migration following focal ischemia and peripheral stimulation in mice. *Dev Neurobiol*. 2008; 68:1474–1486. [PubMed: 18777565]
27. Eisenburger P, Sterz F, Holzer M, Zeiner A, Scheinecker W, Havel C, et al. Therapeutic hypothermia after cardiac arrest. *Curr Opin Crit Care*. 2001; 7:184–188. [PubMed: 11436525]
28. Bronster DJ. Neurologic complications of cardiac surgery: current concepts and recent advances. *Curr Cardiol Rep*. 2006; 8:9–16. [PubMed: 16507229]
29. Wellons JC 3rd, Sheng H, Laskowitz DT, Burkhard Mackensen G, Pearlstein RD, Warner DS. A comparison of strain-related susceptibility in two murine recovery models of global cerebral ischemia. *Brain Res*. 2000; 868:14–21. [PubMed: 10841883]
30. Majid A, He YY, Gidday JM, Kaplan SS, Gonzales ER, Park TS, et al. Differences in vulnerability to permanent focal cerebral ischemia among 3 common mouse strains. *Stroke*. 2000; 31:2707–2714. [PubMed: 11062298]
31. Li Y, Lu Z, Keogh CL, Yu SP, Wei L. Erythropoietin-induced neurovascular protection, angiogenesis, and cerebral blood flow restoration after focal ischemia in mice. *J Cereb Blood Flow Metab*. 2006; 27:1043–1054. [PubMed: 17077815]
32. Fujii M, Hara H, Meng W, Vonsattel JP, Huang Z, Moskowitz MA. Strain-related differences in susceptibility to transient forebrain ischemia in Sv-129 and C57black/6 mice. *Stroke*. 1997; 28:1805–1810. discussion 1811. [PubMed: 9303029]

33. Lee SH, Kim YJ, Lee KM, Ryu S, Yoon BW. Ischemic preconditioning enhances neurogenesis in the subventricular zone. *Neuroscience*. 2007; 146:1020–1031. [PubMed: 17434685]
34. Naylor M, Bowen KK, Sailor KA, Dempsey RJ, Vemuganti R. Preconditioning-induced ischemic tolerance stimulates growth factor expression and neurogenesis in adult rat hippocampus. *Neurochem Int*. 2005; 47:565–572. [PubMed: 16154234]
35. Liu J, Solway K, Messing RO, Sharp FR. Increased neurogenesis in the dentate gyrus after transient global ischemia in gerbils. *J Neurosci*. 1998; 18:7768–7778. [PubMed: 9742147]
36. Maysami S, Lan JQ, Minami M, Simon RP. Proliferating progenitor cells: a required cellular element for induction of ischemic tolerance in the brain. *J Cereb Blood Flow Metab*. 2008; 28:1104–1113. [PubMed: 18319730]
37. Yang HK, Sundholm-Peters NL, Goings GE, Walker AS, Hyland K, Szele FG. Distribution of doublecortin expressing cells near the lateral ventricles in the adult mouse brain. *J Neurosci Res*. 2004; 76:282–295. [PubMed: 15079857]
38. Gotz M. Doublecortin finds its place. *Nat Neurosci*. 2003; 6:1245–1247. [PubMed: 14634654]
39. Amagasaki K, Kaneto H, Heldin CH, Lennartsson J. c-Jun N-terminal kinase is necessary for platelet-derived growth factor-mediated chemotaxis in primary fibroblasts. *J Biol Chem*. 2006; 281:22173–22179. [PubMed: 16760468]
40. Kavurma MM, Khachigian LM. ERK, JNK, and p38 MAP kinases differentially regulate proliferation and migration of phenotypically distinct smooth muscle cell subtypes. *J Cell Biochem*. 2003; 89:289–300. [PubMed: 12704792]
41. Gleeson JG, Lin PT, Flanagan LA, Walsh CA. Double-cortin is a microtubule-associated protein and is expressed widely by migrating neurons. *Neuron*. 1999; 23:257–271. [PubMed: 10399933]
42. Francis F, Koulakoff A, Boucher D, Chafey P, Schaar B, Vinet MC, et al. Doublecortin is a developmentally regulated, microtubule-associated protein expressed in migrating and differentiating neurons. *Neuron*. 1999; 23:247–256. [PubMed: 10399932]
43. Couillard-Despres S, Winner B, Schaubeck S, Aigner R, Vroemen M, Weidner N, et al. Doublecortin expression levels in adult brain reflect neurogenesis. *Eur J NeuroSci*. 2005; 21:1–14. [PubMed: 15654838]
44. Brown JP, Couillard-Despres S, Cooper-Kuhn CM, Winkler J, Aigner L, Kuhn HG. Transient expression of doublecortin during adult neurogenesis. *J Comp Neurol*. 2003; 467:1–10. [PubMed: 14574675]
45. Rao MS, Shetty AK. Efficacy of doublecortin as a marker to analyse the absolute number and dendritic growth of newly generated neurons in the adult dentate gyrus. *Eur J NeuroSci*. 2004; 19:234–246. [PubMed: 14725617]
46. Nacher J, Crespo C, McEwen BS. Doublecortin expression in the adult rat telencephalon. *Eur J NeuroSci*. 2001; 14:629–644. [PubMed: 11556888]

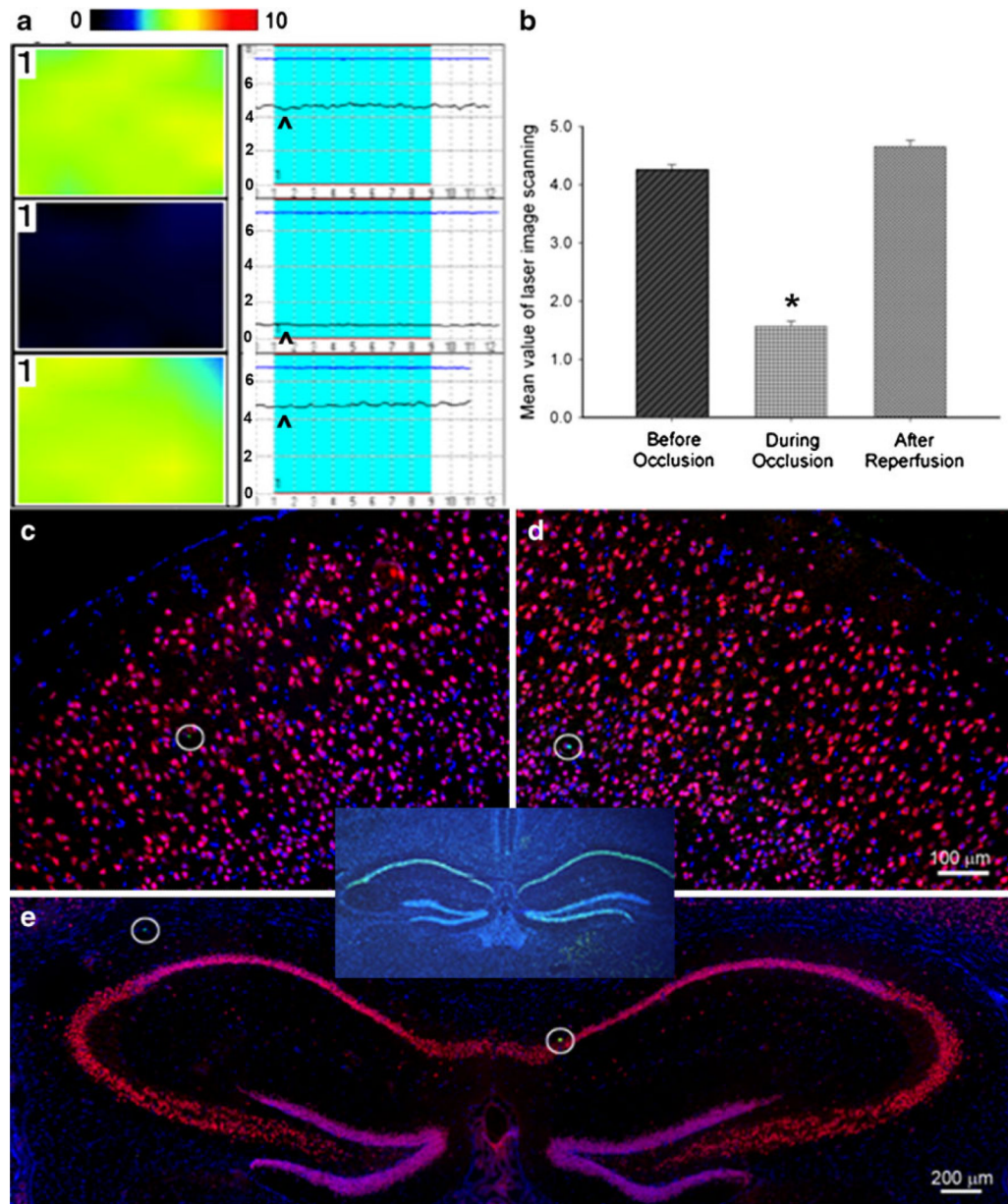


**Fig. 1.** Sublethal global ischemia reduced CBF but did not induce cell death. **a** The laser Doppler scanning images (*left column*) and laser Doppler probe single point measurement (*right column*) show CBF before (*top*), 1 min after (*middle*) CCA occlusion, and right after reperfusion (*bottom*) in the right hemisphere. The color in the laser scanning image represents the level of the blood flow; color standard bar is shown on the top where the blood flow level (*black to red*) stands for 0 to 10 (maximal). In the laser Doppler single point panel, the arrowhead points to the line representing the level of CBF. **b** Average of mean image values in laser scanning imaging at different time points. Cerebral blood flow showed 65% reduction after CCA and restored after reperfusion. \* $P < 0.01$ .  $N = 6$  in each group. **c–e** TUNEL (*green*), NeuN (*red*), and Hoechst 33342 (*blue*) staining 7 days after transient global ischemia showed that there was no delayed neuronal death in either side of the neocortex and hippocampus (**e**). The hollow circles showed TUNEL-positive cells

(*green*) which indicated the natural cell death in the brain. The insert provides a positive control of TUNEL staining, showing massive cell death (*green*) in the hippocampus after an 11-min TGI in C57BL/6 mouse. *Bar*=100  $\mu\text{m}$  in c and d. *Bar*=200  $\mu\text{m}$  in e

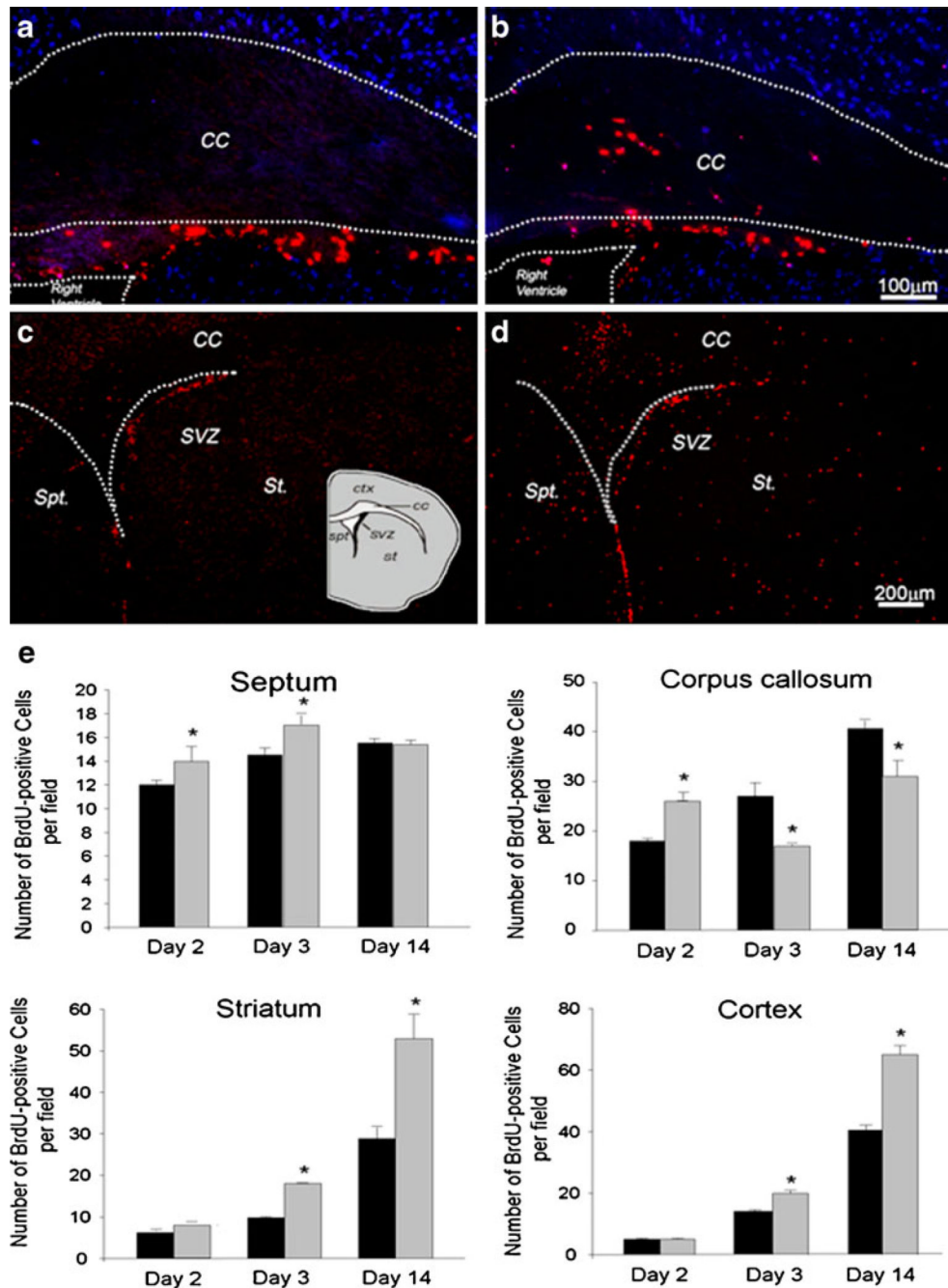


**Fig. 2.** BrdU-positive cells in different brain regions after sublethal global ischemia. BrdU immunostaining for proliferating cells in the SVZ, corpus callosum (CC), septum (Sep), striatum, and cortex. **a, b** More BrdU-positive cells (red) were seen in corpus callosum 1 day after sublethal transient global ischemia (**b**) compared to sham group (**a**). Hoechst 33342 staining (blue) showed cell nuclei. **c, d** The BrdU-positive cells (red) in areas surrounding SVZ (Spt, St, and CC) 7 days after TGI in the sham-operated group (**c**) and the TGI group (**d**). There were more BrdU-positive cells in these areas in TGI animals. **e** BrdU-positive cells were counted and statistically analyzed in Spt, CC, St, and CTX, separately.

The *black bar* represents sham control and *gray bar* represents TGI animals ( $N=6$  in each group). \* $P<0.05$  compared to controls

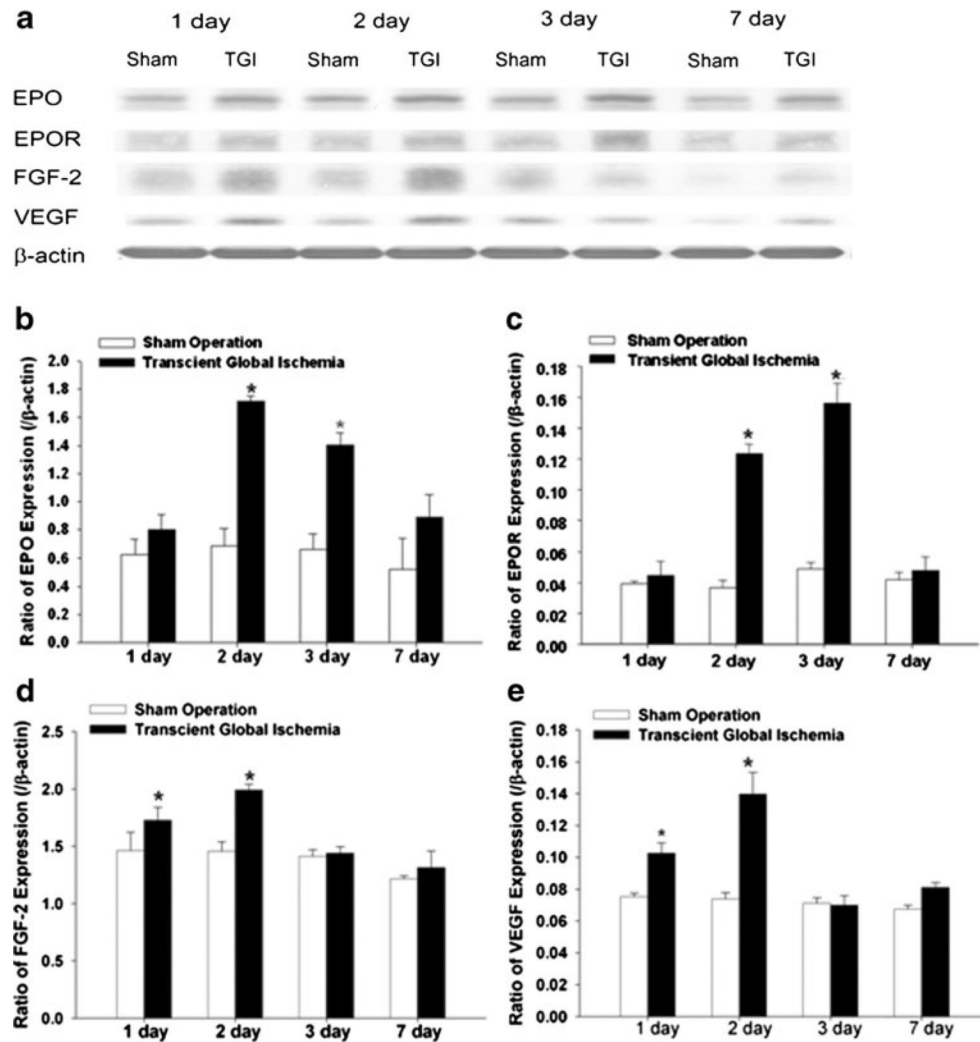


**Fig. 3.** Upregulation of neurotrophic and neurogenetic factors after sublethal TGI. Western blot analysis was performed for both hemispheres to detect expression of EPO, EPOR, FGF-2, and VEGF protein levels at different days after TGI. **a** Representative Western blotting in the neocortex 1, 2, 3, and 7 days after sublethal TGI. Beta-actin was used as loading control. **b–e** Quantification of the expression of neurotrophic and neurogenetic factors EPO (**b**), EPOR (**c**), FGF-2 (**d**), and VEGF (**e**) at different days after the TGI. The gray intensity of corresponding bands was normalized to  $\beta$ -actin.  $N=3$  independent assays in each group at each time point. \* $P<0.05$  compared with controls



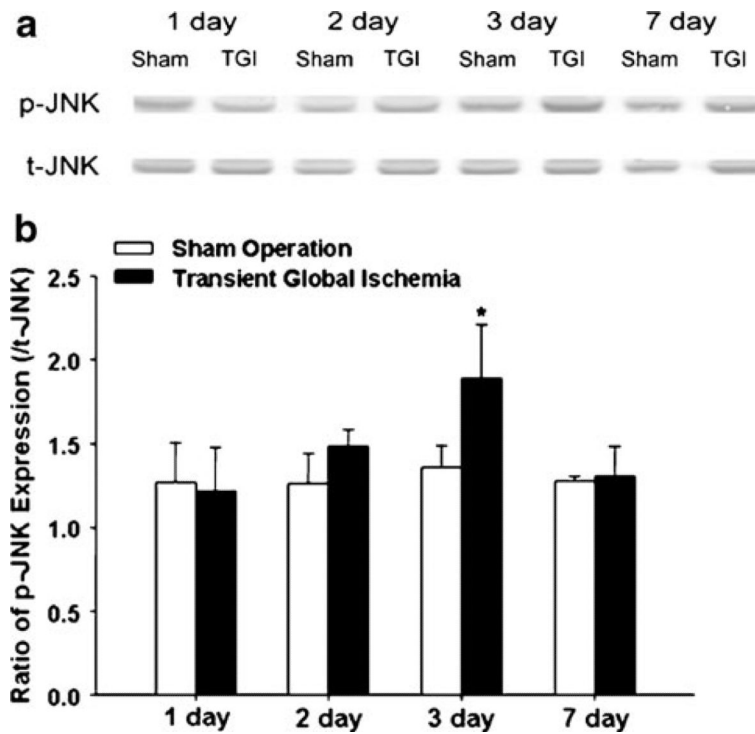


**Fig. 4.** Upregulation of P-JNK after sublethal TGI. JNK and phosphor-JNK (p-JNK) were detected by Western blot in the neocortex 1, 2, 3, and 7 days after sublethal TGI. **a** Representative Western blot gel shows the level changes of JNK and p-JNK at different days after TGI. **b** Quantification of the expression ratio of p-JNK to total JNK 1, 2, 3, and 7 days after TGI. Three days after reperfusion, the expression of p-JNK was significantly higher in TGI group compared to sham group. \* $P < 0.05$  compared to sham group.  $N = 3$  in each group at each time point

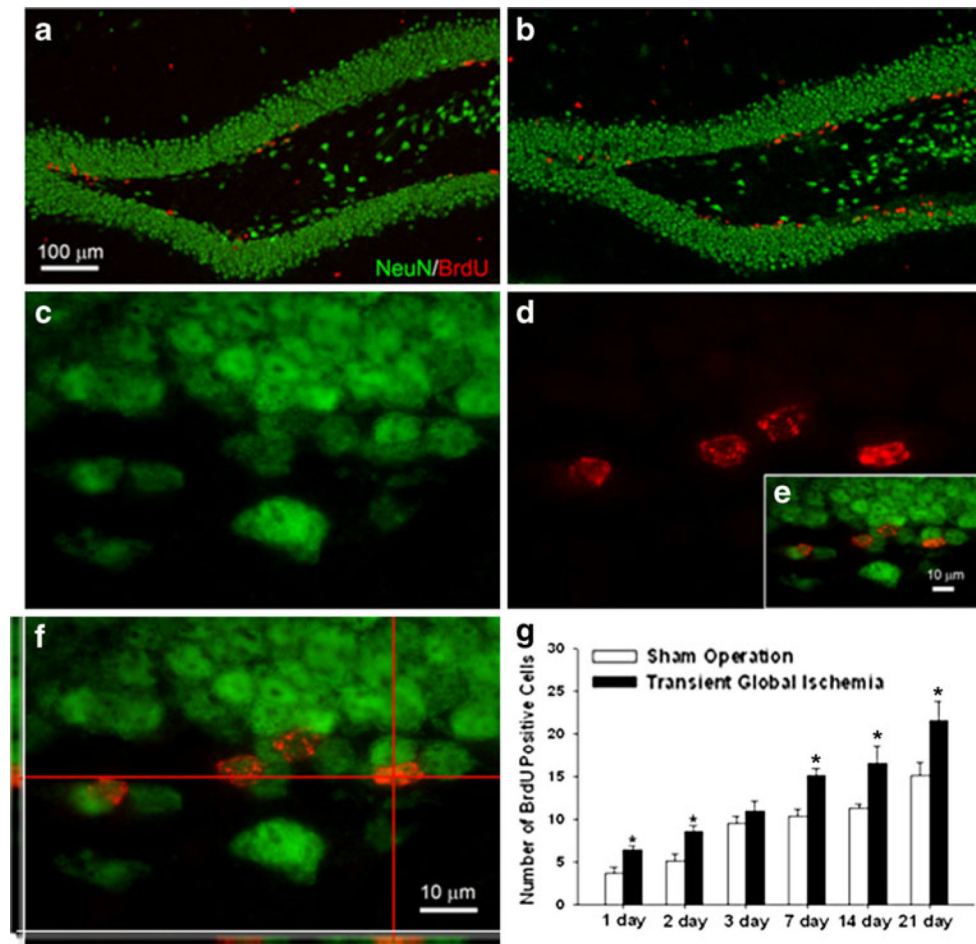


**Fig. 5.** Sublethal global ischemia enhanced neurogenesis in DG. Immunohistochemical staining was applied to detect BrdU-positive cells and colocalization with NeuN. **a, b** More BrdU-positive cells (*red*) were seen in the SGZ in the TGI group (**b**) than in the sham-operated group (**a**) 7 days after ischemia. **c–f** Higher magnification images show NeuN- (**c**) and BrdU-positive (**d**) cells in the dentate gyrus 7 days after TGI. The colocalization of NeuN and BrdU was confirmed by confocal imaging shown in **e** and **f**. Note colocalization of red and green colors in the side images. **g** BrdU-positive cells were quantified 1–21 days after TGI in both ischemia and sham groups.  $N=6$  in each group.  $*P<0.05$  compared to controls. *Bar*=100  $\mu\text{m}$  in **a** and **b**. *Bar*=10  $\mu\text{m}$  in **c–f**

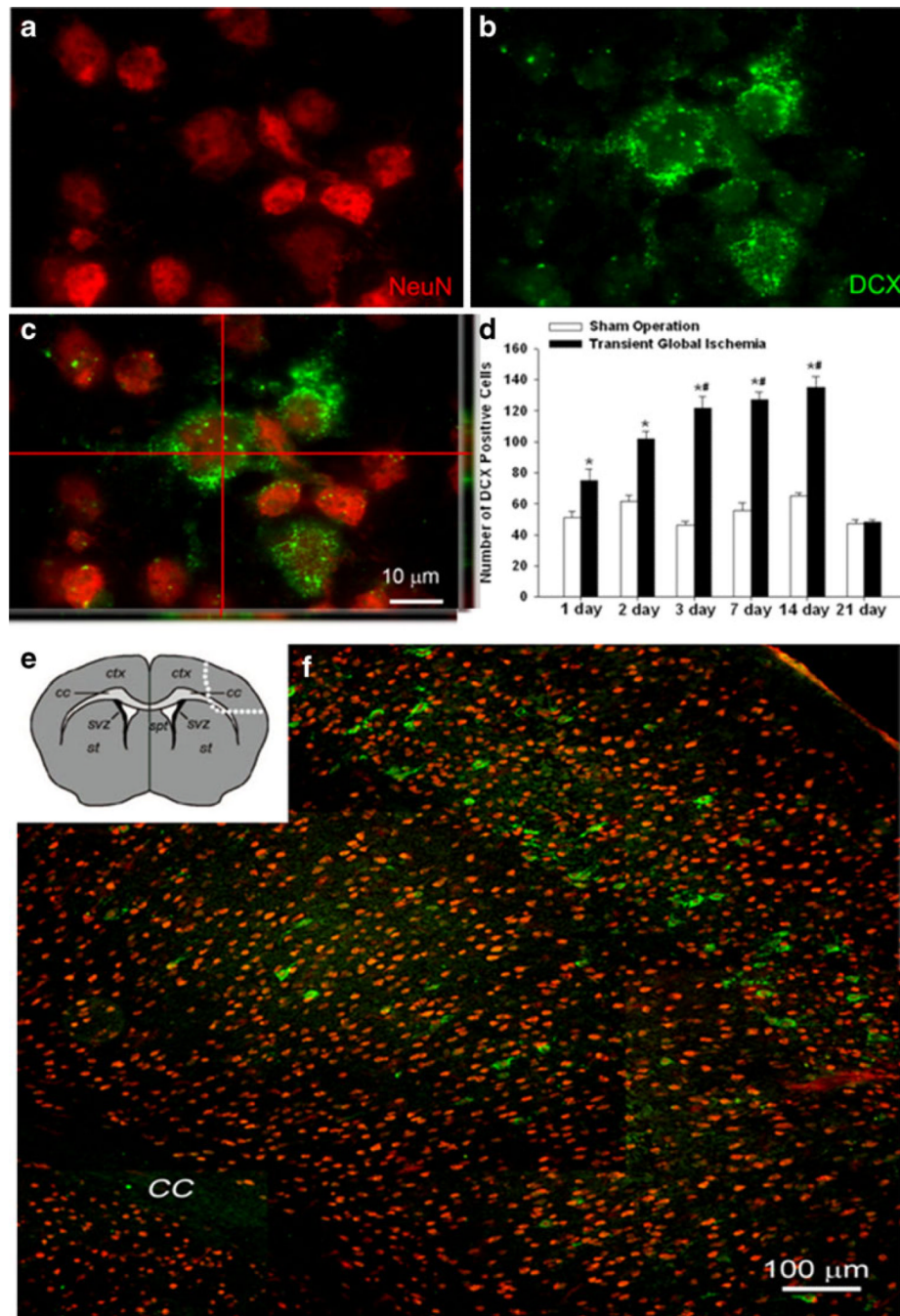


**Fig. 6.** Sublethal global ischemia enhanced DCX-positive cells in the neocortex. Confocal imaging of NeuN and DCX double staining in the neocortex of the control and TGI brain. **a, b** NeuN (red) and DCX (green) labeling, respectively. **c** The confocal image shows overlapping of NeuN and DCX staining. Note the colocalization of red and green colors in the two side images. **d** Quantification of DCX-positive cells in both left and right hemispheres, counted 1–21 days after TGI and compared with sham groups. TGI significantly stimulated DCX expression. By 21 days after TGI, DCX expression subsided. \* $P < 0.05$  compared to control.  $N = 6$  in each group. **e** The diagram shows the area outlined by dotted line where the image **f**

was taken from. **f** DCX-positive cells distributed in the neocortex in the layers I, III, and V.  
*Bar*=10  $\mu$ m in **a–c**. *Bar*=100  $\mu$ m in **f**

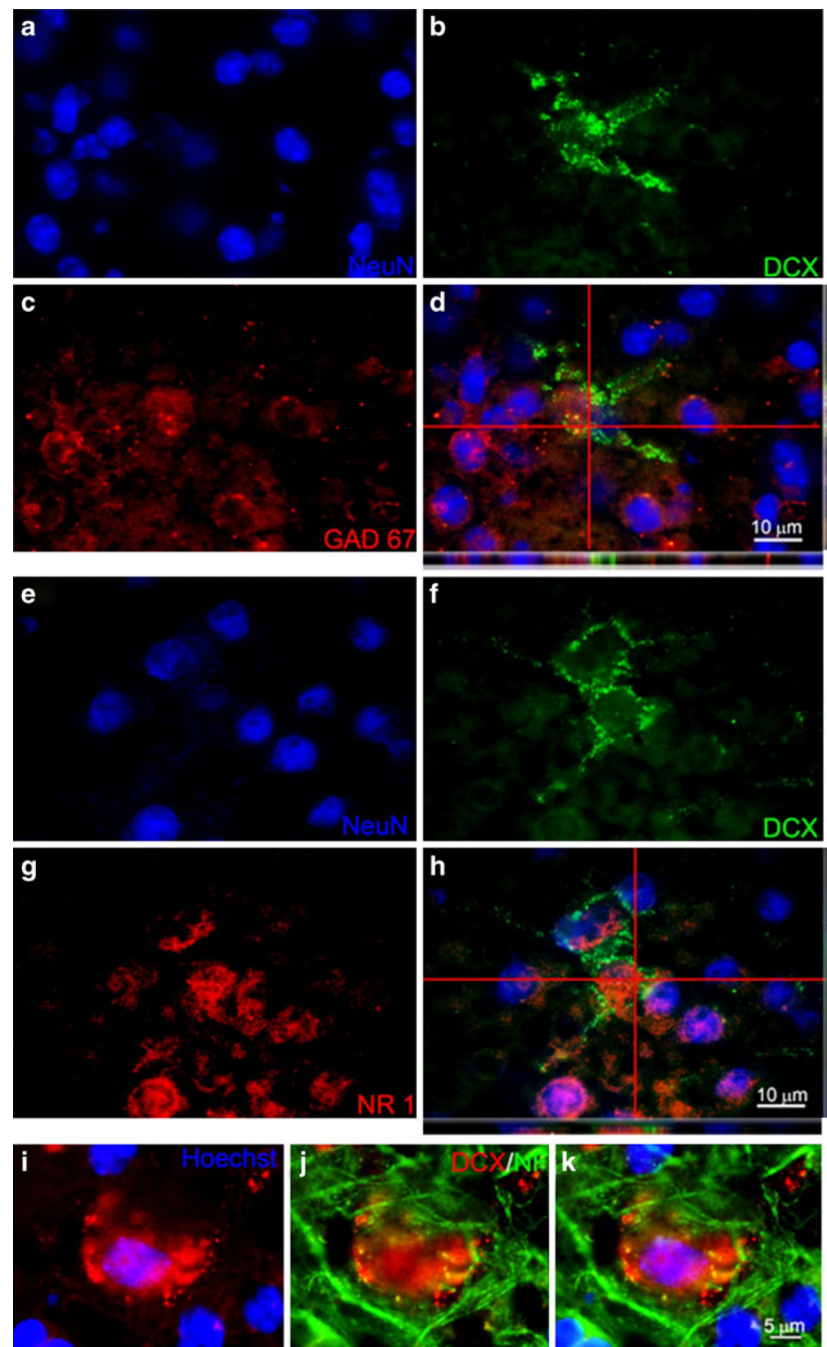


**Fig. 7.** DCX-positive cells colocalized with mature neuronal markers. Confocal imaging analysis of colabeling of DCX and neuronal markers in the neocortex 7 days after TGI. **a–c** NeuN (*blue*), DCX (*green*), and GAD67 (*red*) staining, respectively. **d** The three-dimensional confocal image shows colabeling of NeuN and the GABAergic neuronal marker GAD67. Note the colocalization of green and red colors in side images. **e–g** NeuN (*blue*), DCX (*green*), and NR1 (*red*) staining, respectively. **h** The confocal image shows colocalization of DCX with the glutamatergic NMDA receptor gene NR1. **i–k** Enlarged images showed that DCX (*red*) colocalized with another mature neuronal marker neurofilament (*NF*; *green*). *Bar*=10 μm in **a–h**. *Bar*=5 μm in **i–k**